RI 9066

Bureau of Mines Report of Investigations/1987

Pillar Load Transfer Associated With Multiple-Seam Mining

By R. J. Matetic, G. J. Chekan, and J. A. Galek

UNITED STATES DEPARTMENT OF THE INTERIOR

Pillar Load Transfer Associated With Multiple-Seam Mining

By R. J. Matetic, G. J. Chekan, and J. A. Galek

CONTENTS

ILLUSTRATIONS

TABLES

```
            UNIT OF MEASURE ABBREVIATIONS USED IN THIS REPORT

ft      foot                    psi/ft      pound per square inch per foot

in      inch                    psig        pound per square inch, gauge

pct     percent                 yr          year

psi     pound per square inch
```

PILLAR LOAD TRANSFER ASSOCIATED WITH MULTIPLE-SEAM MINING

By R. J. Matetic,[1] G. J. Chekan,[1] and J. A. Galek[2]

ABSTRACT

The Bureau of Mines, as part of a program to improve mine planning and development, is currently investigating the effects of pillar load transfer, which can impact mining operations within a multiple-seam configuration. At two mine sites where such ground interactions were present, the Bureau performed a complete geological analysis and installed and monitored instrumentation to gather pertinent data on rock mechanics. Overburden depth varied dramatically in the vicinity of the study area and reached a maximum at the study site; innerburden thickness was less than a pillar width (40 to 45 ft); heaving was experienced in both mines where sandstone and/or shale floor units were observed; overlays of the mine layouts show pillars were not totally superpositioned; a maximum of 5 in of roof to floor convergence was measured; and pressure readings indicated pillar core loading only and increased to a maximum of 7,000 psig over instrument setting pressure.

INTRODUCTION

The simultaneous mining of coalbeds lying one above another is widely practiced throughout the Appalachian Region of the Eastern United States. Strata interaction effects represent a major problem associated with this type of mining. Pillar load transfer is an interaction that occurs as a result of load transfer through pillars in overlying or underlying mining operations. Such interactions can be classified by the geologic environment and those that depend on engineering design (1).[3] These engineering design variables include: pillar dimensions and geometries, mining height, mining method, entry span, and age of workings.

---

[1]Mining engineer.
[2]Engineering technician.
Pittsburgh Research Center, Bureau of Mines, Pittsburgh, PA.
[3]Underlined items in parentheses refer to items in the list of references at the end of this report.

FIXED PARAMETERS

The fixed parameters include depth, innerburden thickness, and innerburden physical characteristics. The innerburden is defined as the material, consolidated or unconsolidated, that lies between deposits of useful materials, ores or coal. The mine design parameters include seam sequencing and columnization of pillars. The overall understanding of pillar load transfer and its effect on seam interaction is limited. Few attempts have been made to correlate these variables in relation to underground instrumentation and monitoring. The Bureau conducted this study to develop a better understanding of pillar load tranfer and its effects on current workings. Eventually, this knowledge will lead to improvements in mine planning and development.

MINE LOCATION AND GEOLOGY

The study mines are located in Raleigh County, WV, as shown in figure 1. The company is operating in two superimposed coalbeds. The upper mine is located in the Peerless Coalbed, which is approximately 72 in thick. The lower mine is located in the No. 2 Gas Coalbed, which is approximately 48 in thick. The mines are separated by approximately 40 to 45 ft of innerburden.

A generalized stratigraphic column of the study area is shown in figure 2. The overburden consists predominantly of sandstone with innerbedded shale units of varying thickness. The innerburden also consists of a predominant sandstone with some innerbedded shale units.

DEPTH

Depth in relation to all room-and-pillar mining operations is critical as overburden increases (1). Figure 3 is an overburden isopach map showing overburden depth in relation to the study site for the lower mine. The overburden above the lower mine at the study site is approximately 1,000 ft thick, the innerburden is approximately 40 ft thick, and approximately 960 ft of cover is located above the study site in the upper mine. To understand the effect of depth, a plot was constructed of upper seam depth versus innerburden thickness. A theoretical cutoff is shown on the plot to demonstrate the effect of increasing depth on

FIGURE 1.—Location of study mines.
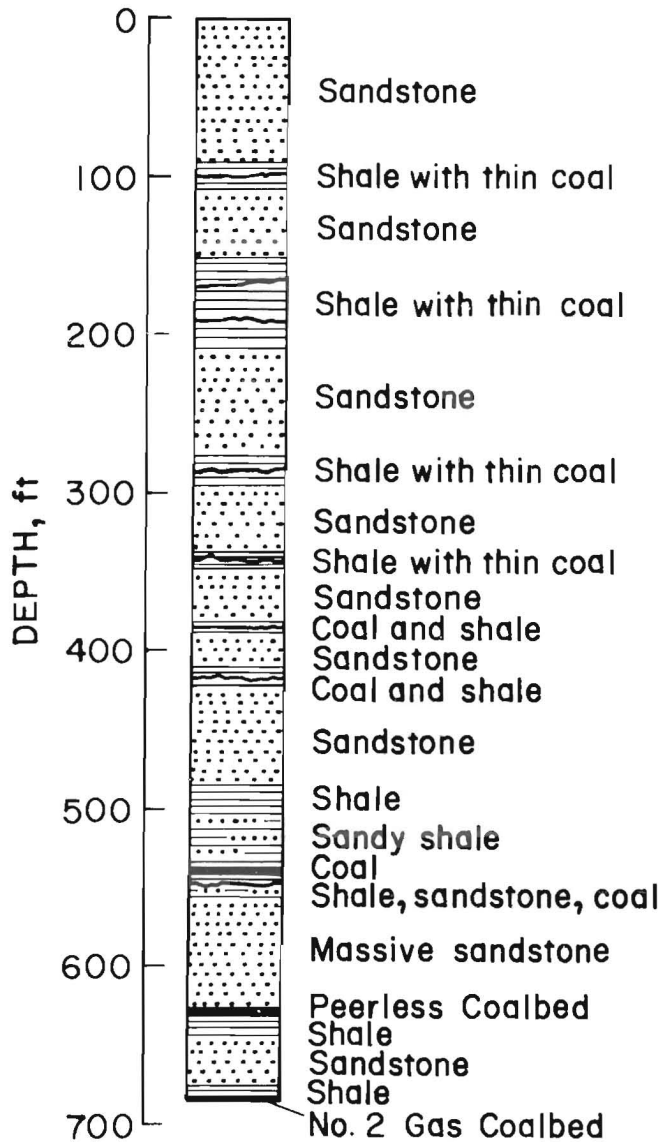
FIGURE 2.—Generalized stratigraphic column of study area.

The stratigraphic column shows, from top (0 ft) to bottom (700 ft):

- Sandstone
- Shale with thin coal (~100 ft)
- Sandstone
- Shale with thin coal (~175 ft)
- Sandstone
- Shale with thin coal (~275 ft)
- Sandstone
- Shale with thin coal
- Sandstone
- Coal and shale
- Sandstone
- Coal and shale
- Sandstone
- Shale (~480 ft)
- Sandy shale
- Coal
- Shale, sandstone, coal
- Massive sandstone
- Peerless Coalbed
- Shale
- Sandstone
- Shale
- No. 2 Gas Coalbed (~700 ft)

mine opening stability (fig. 4) (1). As shown in the figure, at a depth of 960 ft and an innerburden spacing of 40 ft, the upper mine is well within the unstable region. It should be noted that the plot is not necessarily conclusive due to a shortage of information regarding greater depths with larger innerburden intervals (1). Also, this graph does not consider pillar or entry design.

INNERBURDEN THICKNESS AND PHYSICAL CHARACTERISTICS

Interval thickness between two coalbeds is also a critical variable. Pillar load transfer from overlying workings represents a major problem, especially where the two seams are fairly close together (2). Figure 5 is an innerburden isopach map constructed from available corehole information. Approximately 43 ft separates the upper and lower mines at the study site.

Through available core logs, figures 6 and 7 demonstrate innerburden profiles along a northeast and northwest trend with respect to the study area. According to these figures, the sandstone percentage located within the innerburden averages 77 pct.

Figure 8, constructed from 25 room-and-pillar case studies (2), displays a relationship between innerburden thickness and interactive distance. According to Haycocks (2), and using the equation

$$I = 110 - 0.42S, \qquad (1)$$

where I = innerburden spacing in feet above which no interaction damage may be expected from room-and-pillar mining,
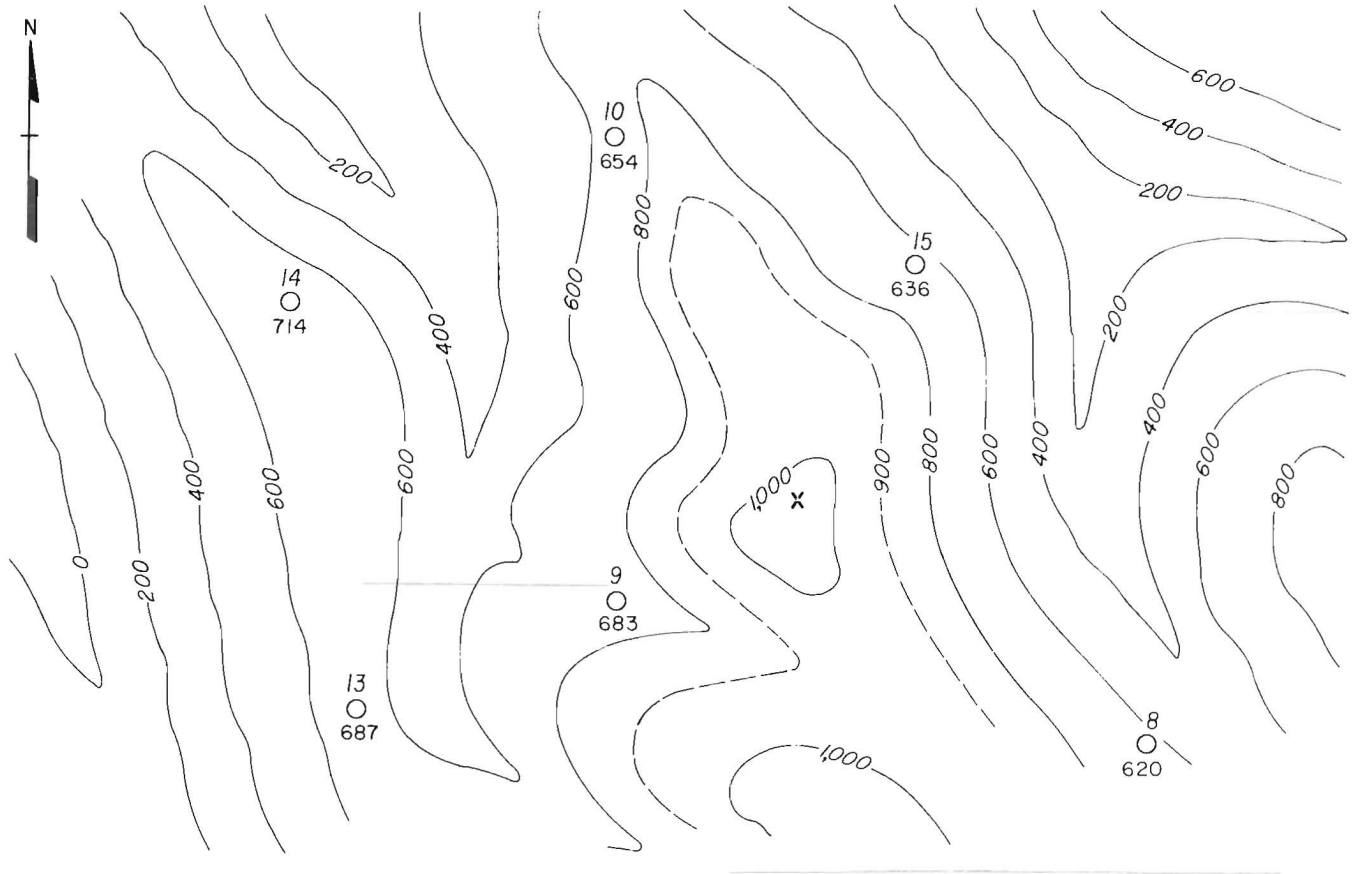
LEGEND

10 Drill hole (top number:
O   identification, bottom:
654   depth, ft)

Contour interval = 200 ft

X Instrumented pillar

0   800

Scale, ft

FIGURE 3.—Overburden isopach map of lower mine.

5
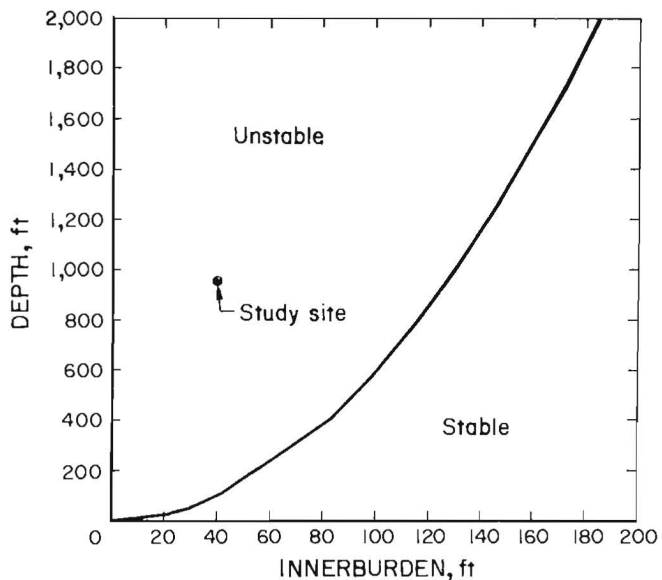
FIGURE 4.—Upper seam depth versus innerburden thickness in upper mine. Adapted from C. Haycocks, B. Ehgartner, M. Karmis, and E. Topuz (1).
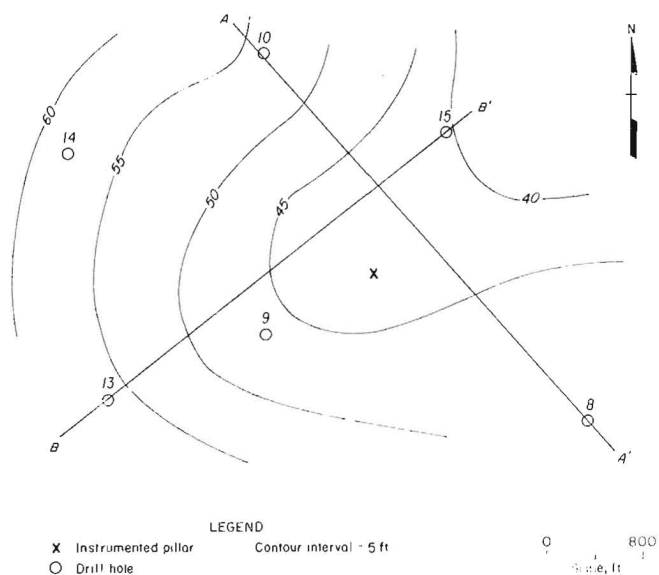
FIGURE 5.—Innerburden isopach map. A-A' and B-B' locate profiles shown in figures 6 and 7.

LEGEND
Shale
Sandstone
Coalbed
15 Drill-hole number
A-A' Section shown in figure 5
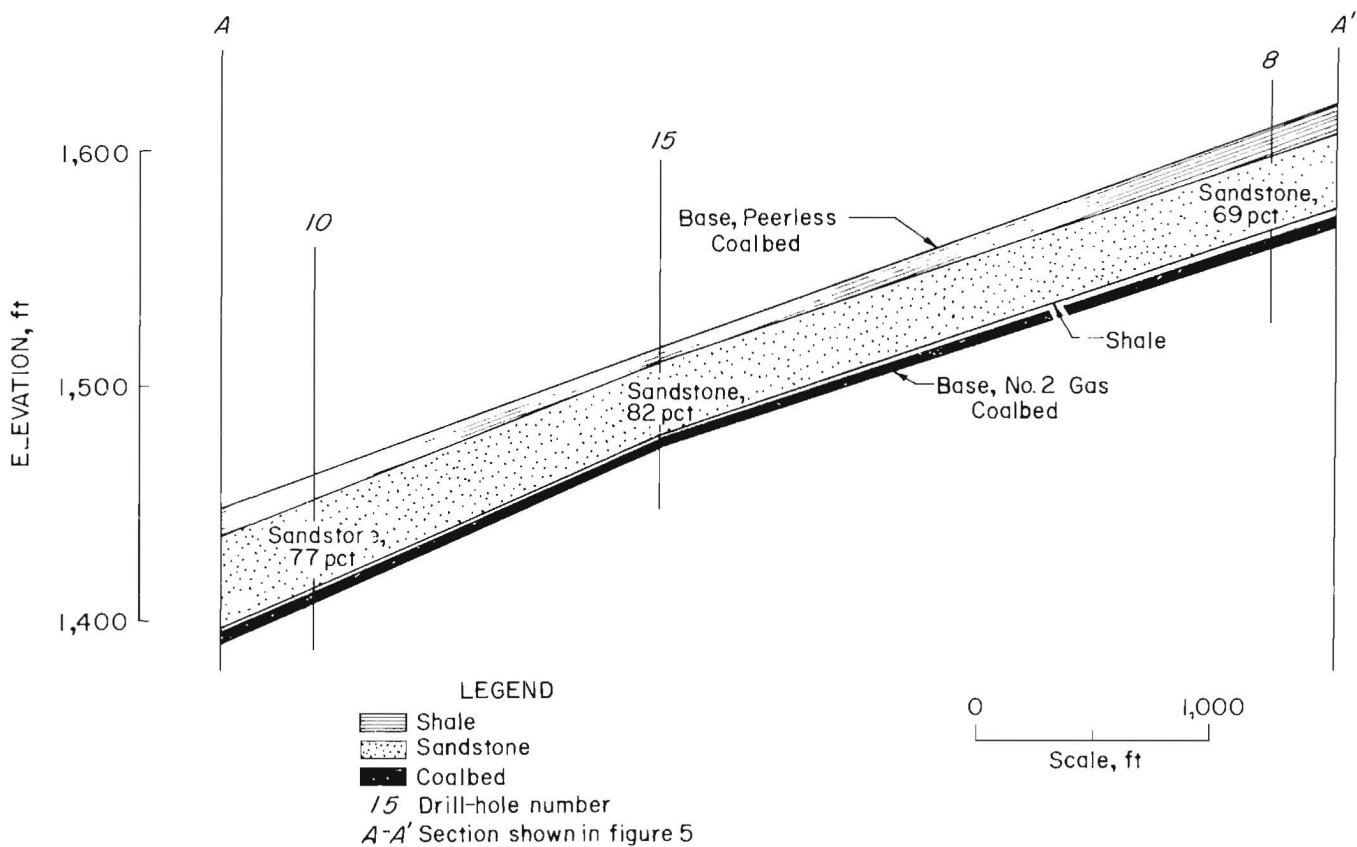
FIGURE 6.—Innerburden profile along northeastern trend through study area.
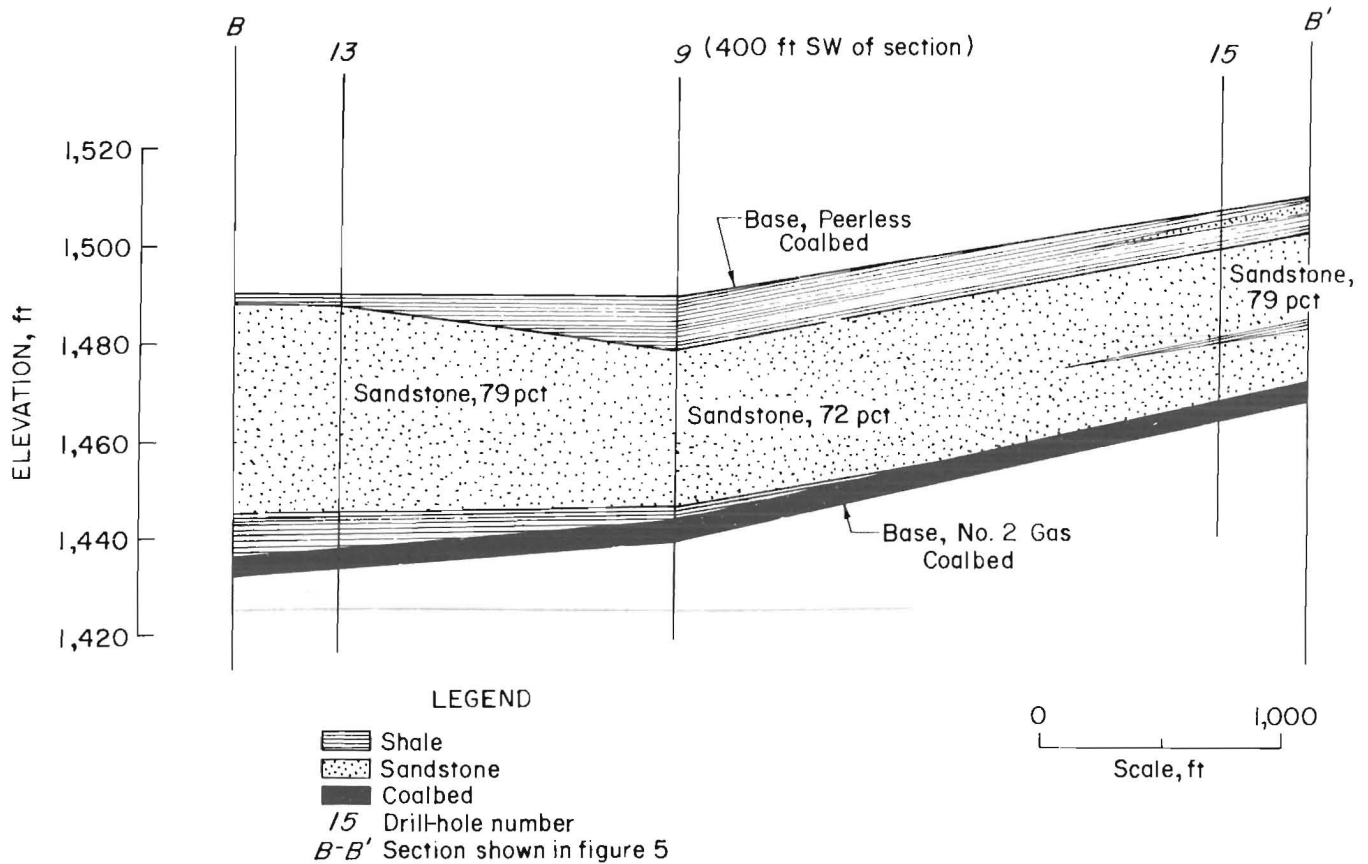
FIGURE 7.—Innerburden profile along northwestern trend through study area.
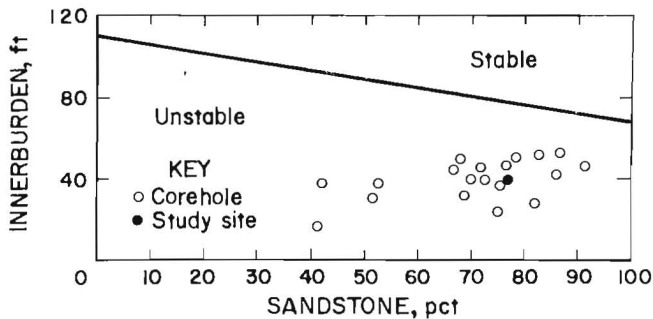
FIGURE 8.—Innerburden thickness versus percent sandstone. Adapted from C. Haycocks and M. Karmis (2).

and   S = sandstone percentage located within the innerburden,

a limit on interactive distance could be obtained based on the lithology of the innerburden.

By substituting the sandstone percentage of 77 pct into equation 1, the interactive distance is calculated as

$$I = 110 - 0.42(77)$$

$$= 78 \text{ ft.} \qquad (2)$$

According to Haycocks (2), approximately 78 ft would be the innerburden spacing above which no interaction damage may result from room-and-pillar mining. The actual innerburden, with respect to the study site, is approximately 40 ft, considerably less than the calculated minimum value. Figure 8 shows location of the study site with respect to innerburden spacing versus percent sandstone. As shown, the study site is again located within the unstable region. Core logs,

provided from the company, are also shown in the figure. It is interesting to note that the data from all core logs fell within the unstable range. Also, these graphs are independent of pillar and entry design and are derived from a rather limited data set. Therefore, this may not represent all stable and/or unstable mining conditions.

Ehgartner (3) used photoelastic models to determine if the degree of layering within the innerburden is a function of interactive distance. Figure 9 shows a plot of innerburden thickness versus number of innerbeds for the study site with respect to the information developed by Ehgartner (3). One sandstone and two shale zones are the three units identified within the innerburden. With three innerbeds and an innerburden thickness of approximately 40 ft, the study site falls within the unstable range. Interval thickness and the number of innerbeds from all available core logs were also plotted in the figure. Note that all corehole data fell within the
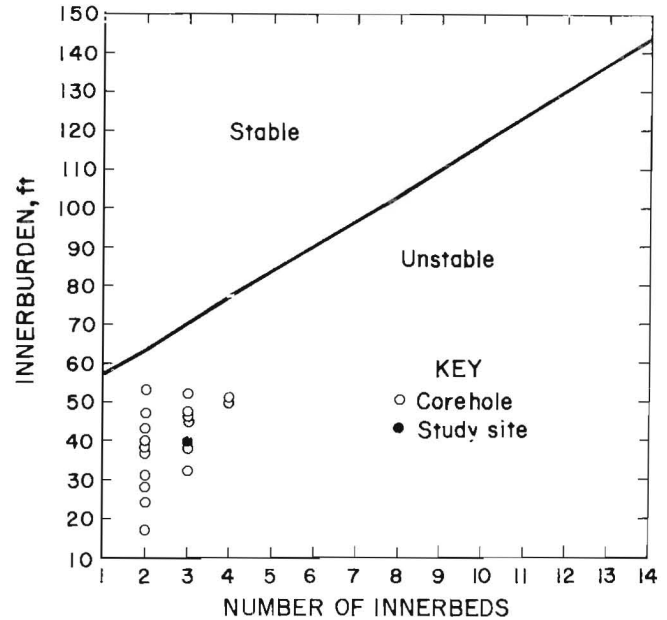
FIGURE 9.—Innerburden thickness versus number of innerbeds. Adapted from B. Ehgartner (3).

unstable range. This figure was also constructed utilizing a limited data set.

RESULTS OF IN-MINE MAPPING

A geologic investigation was performed within both the upper and lower mines. In-mine mapping was conducted to observe and measure roof and floor lithology, roof joint orientation, cleat orientation, and any discontinuities that might be present. The areas of floor heave in both mines were underlain by a rooted, fine-grained, well-cemented, hard sandstone and/or shale, and the roofs consisted of either a hard, banded siltshale or sandstone. Roof structure was generally uniform except for some slight undulations in the shale-sandstone contact. The coal cleat orientation was not easily determined because of the presence of abundant microfractures and pillar sloughing. No joints in the roof could be detected, although pronounced jointing

did occur in an outcrop at the mine portal. The immediate roof rock in the heave zones of the lower mine appeared to be sandstone. In areas where a shale roof was observed, no floor heave was detected. The heave zones in the upper mine could not be correlated to roof-rock lithology since sandstone was present throughout.

Figures 10 and 11 represent the results of the in-mine mapping. Figure 10 shows the location of floor heave around the study site in the upper mine. Note the mine roof is chiefly sandstone near the study area, and the floor is comprised of hard, fine-grained, rooted sandstone. Figure 11 represents the results of the floor heave around the study site within the lower mine. The immediate floor

8
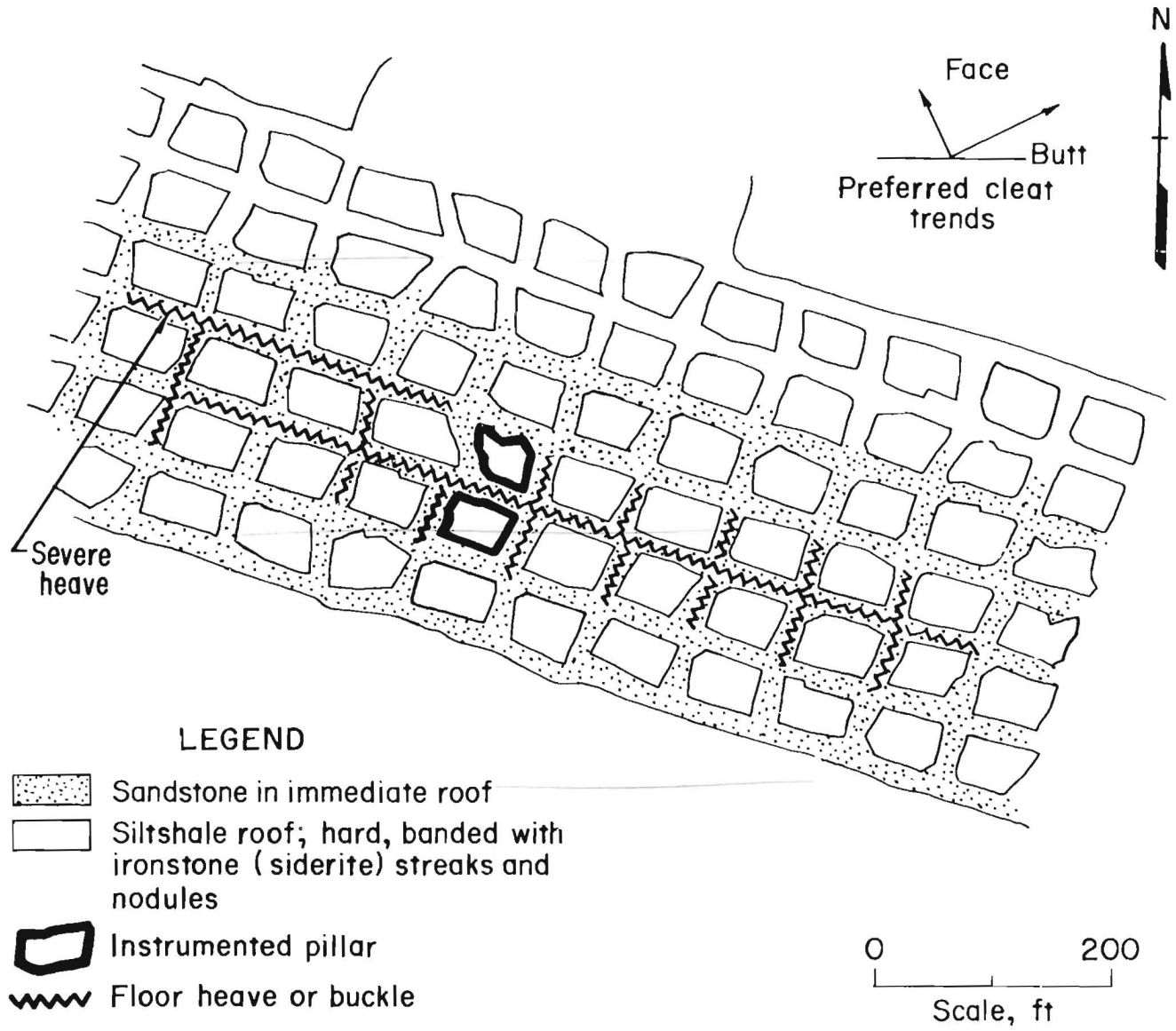
FIGURE 10.—Results of in-mine mapping of upper mine.

LEGEND

Sandstone in immediate roof

Siltshale roof; hard, banded with ironstone (siderite) streaks and nodules

Instrumented pillar

Floor heave or buckle

Face

Butt

Some common
cleat trends

Not
accessible

Sandstone roll

N

Buff
sandstone

Gray
sandstone

Silt-
shale

LEGEND

Sandstone in immediate roof

Siltshale roof; hard, banded with
ironstone (siderite) streaks and
nodules

Instrumented pillar

Floor heave or buckle

Mine track

0   200
Scale, ft

FIGURE 11.—Results of in-mine mapping of lower mine.
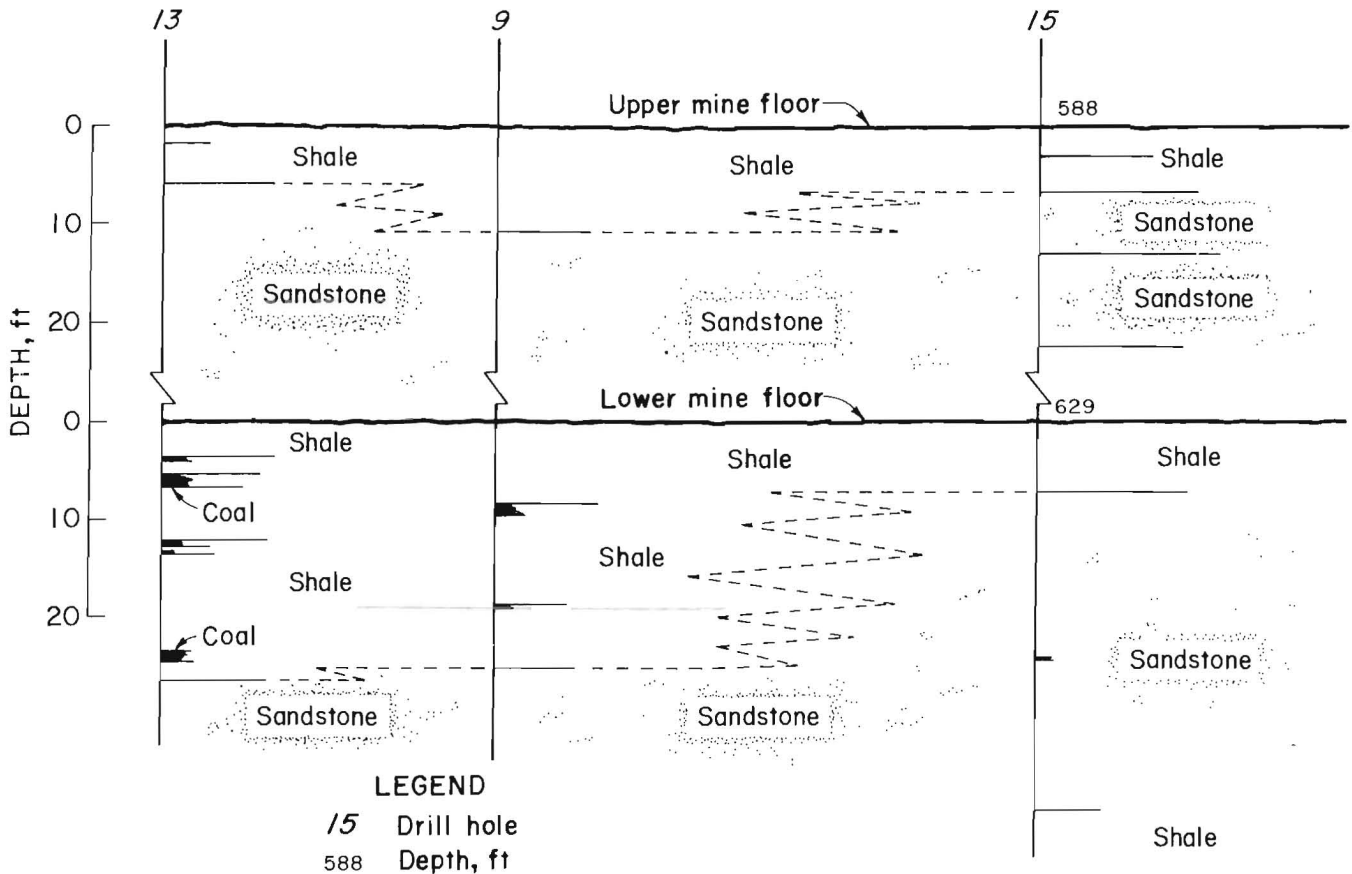
FIGURE 12.—Floor lithology in study site area.

located within the heave zones is also comprised of sandstone. Heave zones located in shale floor were found and also demonstrated "hump-like" structures. The transfer of load from a shale to a sandstone unit could be related to the ground conditions located within the lower mine. Figure 12 was constructed from core logs and displays floor lithology in the area of the study site. Note the lateral changes in the immediate floor lithology. The immediate floor is comprised of both a high-modulus material (a sandstone), and a low-modulus material (a shale).

In the heaving experienced near the study site, there was a sandstone floor. Inby or outby the study site, major floor heaving was experienced where a shale floor was present. Floor heaving experienced in these areas resembled "hump-like" structures characteristic of a low-modulus material. A buckling type of failure was also observed where a sandstone floor was present. It may be assumed that major concentrations of load can be transferred from a shale (low-modulus material) to a sandstone (high-modulus material), which may result in movement within the sandstone floor.

MINING ENGINEERING DESIGN PARAMETERS

SEAM SEQUENCING

Finlay and Winstanley (4) state, "Experience has shown that whether the upper or lower seam was worked first, the subsequent working of the other seam in the same area seriously affected the roads in the seam first worked." There are only four possible mining sequences (2):

1. The upper seam is mined out before mining of any underlying seam.

2. Both seams are mined simultaneously, and both are coordinated with one another.

3. The lower seam is mined out first before mining any superincumbent seam.

4. Any combinations of the above (5-7).

Depending on which mining sequence is utilized, stress concentrations that can affect the lower seam may be passive when the upper seam is mined out first, and active when other mining sequences are carried out (1). Load concentration and transfer through pillars in overlying operations can occur when the upper seam is mined first and some pillars are left unmined. Typical problems that occur in workings within the lower seam when this type of sequencing is utilized include floor heave, pillar crushing and failure, rib spalling, and roof failure (8-12). The upper mine area was driven in June 1980, and the same section located in the lower mine was driven during December 1982. Major floor heaving and excessive pillar loading were observed within the lower mine in October 1984. Three to four months later, the upper mine experienced excessive entry convergence and pillar loading. Figures 13 and 14 show conditions that were observed at the study site within the lower mine. As shown, major floor heaving, rib spalling, pillar crushing, and failure occurred. Although very difficult to perform, the ideal solution to eliminate these problems would be to totally extract each seam leaving no pillars, starting with the uppermost seam and then continuing downwards. Very few field studies have been conducted that document this pillar load transfer phenomenon; however, researchers have found that this theory correlates well with relatively successful mining practice (2).

FIGURE 13.—Major floor heaving and rib spalling occurring in lower mine.
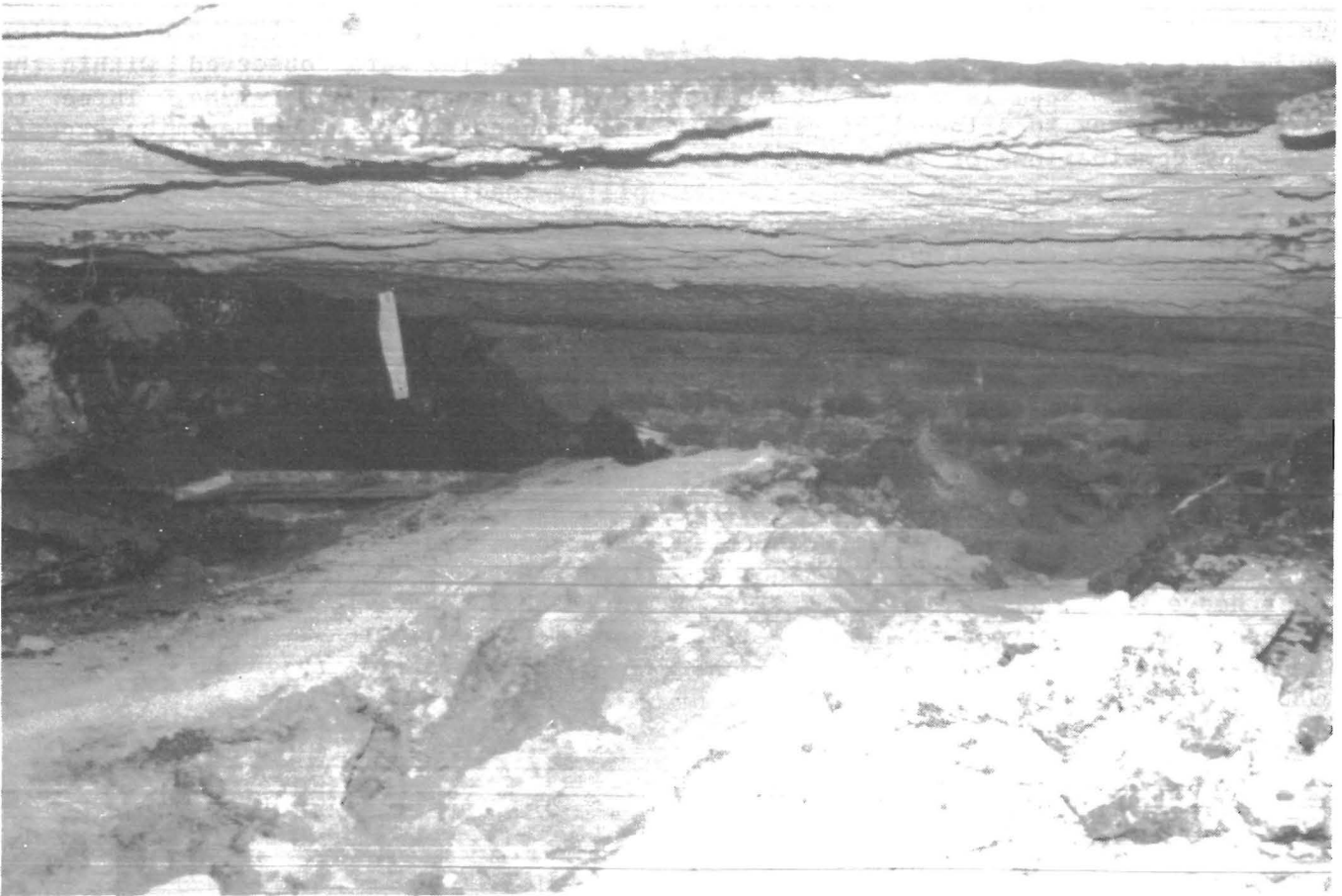
FIGURE 14.—Major floor heaving occurring in lower mine.

SUPERPOSITIONING OF PILLARS

The use of columnized pillars is standard practice in multiple-seam mine design. Columnization of the pillars lessens the effect of interaction that may be transferred from overlying workings. Figure 15 represents the superpositioning of pillars at the study site. Although very difficult to achieve, this practice requires alignment of pillars of similar size and shape for both seams. Both the upper and lower mines were driven with pillars on 70-ft centers. Note (fig. 15) that pillars and entries are nearly, but not totally, superpositioned. Peng and Chandra (13) developed a simplified model representing pressure interaction between columnized pillars, as shown in figure 16. A uniform loading of the overburden is shared equally by the upper seam pillars and, in return, they transmit the load to the floor. Although the pressure transmitted to the pillars is uniform, the load transmitted to the floor is not. A higher pressure develops within the plane where the pillar meets the floor. This pressure decreases downward and dissipates at a distance approximately four

FIGURE 15.—Superpositioning of instrumented pillars.

times the pillar width. The pressure contours shown in figure 16 simulate bulbs. These same contour lines are expected to be in the roof immediately above a pillar (13). If the seam interval is less than eight times the pillar width, the pressure contour lines interact with respect to two superimposed pillars. The assumed pressure between superimposed pillars would be the sum of the two pressure contour lines. The

smaller the interval is between coalbeds, the larger the sum of resulting pressure. Additional pressure can be created from neighboring pillars, but a horizontal dissipation of pressure is minimized when workings are separated by less than two pillar widths (2). The total pressure from these interactions, along with their geomechanical properties, determines whether the strata between the seams will fail or not.

INSTRUMENTATION AND RESULTS

INSTRUMENTATION

Instrumentation installed in both mines included borehole platened flatjacks (BPF) (14) and removable convergence stations. The pillars selected for the study, as shown in figure 15, are nearly superpositioned and have equivalent dimensions.

Borehole platened flatjacks can measure relative increases in pillar pressure, but not actual pillar pressure. The BPF's are calibrated in the laboratory and installed in the coal pillar with a setting pressure equal to the pillar pressure as calculated using the tributary area method (TAM). This method utilizes such factors as overburden

depth, innerburden thickness, and percent extraction.

Removable convergence stations measure roof to floor convergence. Two reference pins are installed in the entry (one in the roof and one in the floor), and subsequent convergence is measured using a removable tube extensometer.

A total of 4 BPF's and 12 convergence stations were installed in the upper mine (fig. 17). A BPF at 30 ft and one at

KEY

W_P Pillar width
W_E Entry width
$\Delta\sigma_Z$ Vertical stress due to pillar loading
σ_P Average pillar loading
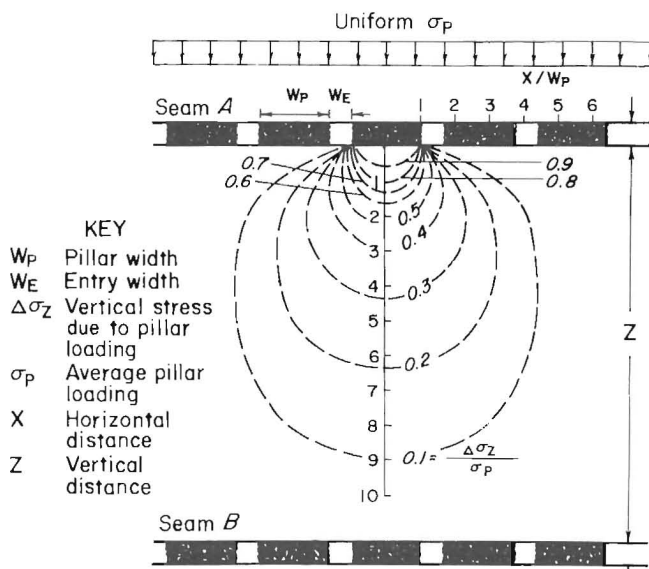X Horizontal distance
Z Vertical distance

FIGURE 16.—Pressure-bulb analysis. Adapted from S. Peng and U. Chandra (13). Influence bulbs are 0.1-0.9 and all numbers on both the x and z axis represent one-half a pillar width.

LEGEND
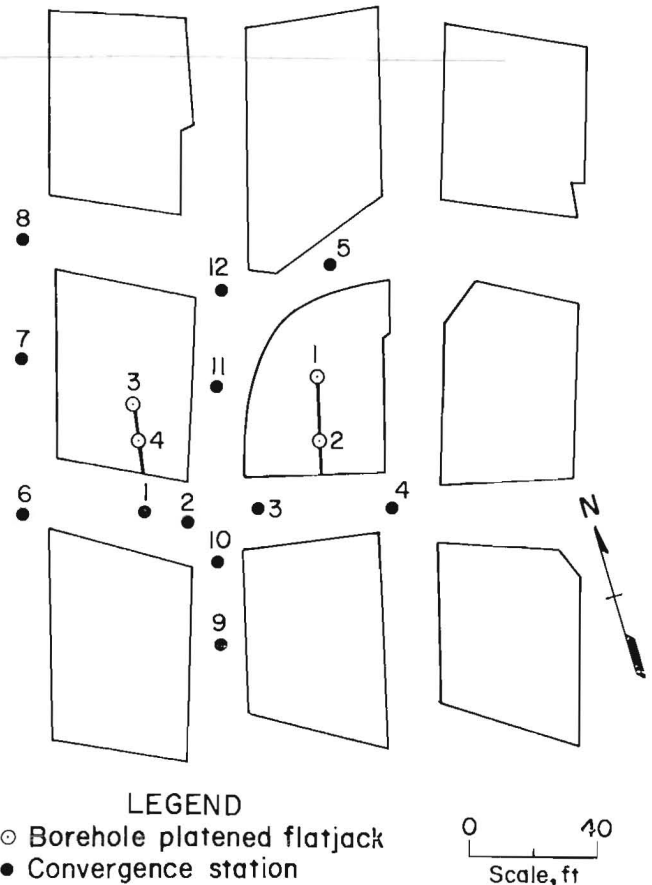⊙ Borehole platened flatjack
● Convergence station

FIGURE 17.—Instrument location in upper mine.

10 ft were installed in the pillar on the right side of the track entry, and BPF's at 21 and 10 ft were installed in the pillar on the left side of the track entry. Owing to the conditions present within the upper mine, BPF 3 was installed at a depth of 21 ft. The locations of the 12 convergence stations are also shown in figure 17.

A total of 5 BPF's and 12 convergence stations were installed in the lower mine, as shown in figure 18. Three BPF's were installed at depths of 30, 10, and 2 ft. A BPF at 30 ft and one at 10 ft were also installed in the adjacent pillar. The estimated setting pressures, using the TAM, were calculated to be 1,200 psig in the upper mine and 1,300 psig in the lower mine. Actual setting pressures are shown in table 1. At the time of installation, setting pressures were determined from information provided using an overburden of 700 ft above the upper mine.

Through the construction of an overburden isopach map (fig. 3), the overburden

LEGEND
○ Borehole platened flatjack
● Convergence station

0   40
Scale, ft

FIGURE 18.—Instrument location in lower mine.

TABLE 1. - Flatjack (BPF) setting pressures, pounds per square inch

BPF	Pressure
Upper mine:	
1	1,100
2	1,225
3	1,200
4	1,275
Lower mine:	
5	1,300
6	1,000
7	1,300
8	1,300
9	1,200

depth was observed to be larger than the original figure. Figure 3 shows the approximate overburden depth above the upper mine to be 960 ft. Therefore, with 40 ft of innerburden, the lower mine experienced an overburden depth of approximately 1,000 ft. Using the TAM and overburden depths of 960 and 1,000 ft for both mines respectively, setting pressures for the BPF's should have been 2,110 psig for the upper mine and 2,200 psig for the lower mine. Although the original setting pressures were low, these pressures do not directly affect the recorded results. It is also safe to assume that any increase in pillar pressure above 2,110 and 2,200 psig would be a result of relative increases in pillar pressure. A complete analysis of setting pressures using the TAM and the monitoring of peak pressures of the nine BPF's will be discussed in further detail in the Innerburden Pressure Analysis section.

RESULTS

The monitoring of the instrumentation continued for a total of 177 days. The instruments were monitored at least once a week. Tables 2 and 3 provide results after 44 days (25 pct of study period), 88 days (50 pct of study period), and 177 days (100 pct of study period).

Table 2 displays the BPF data. BPF 1 and BPF 3, both located in the upper mine at depths of 30 and 21 ft respectively, displayed major increases in pillar
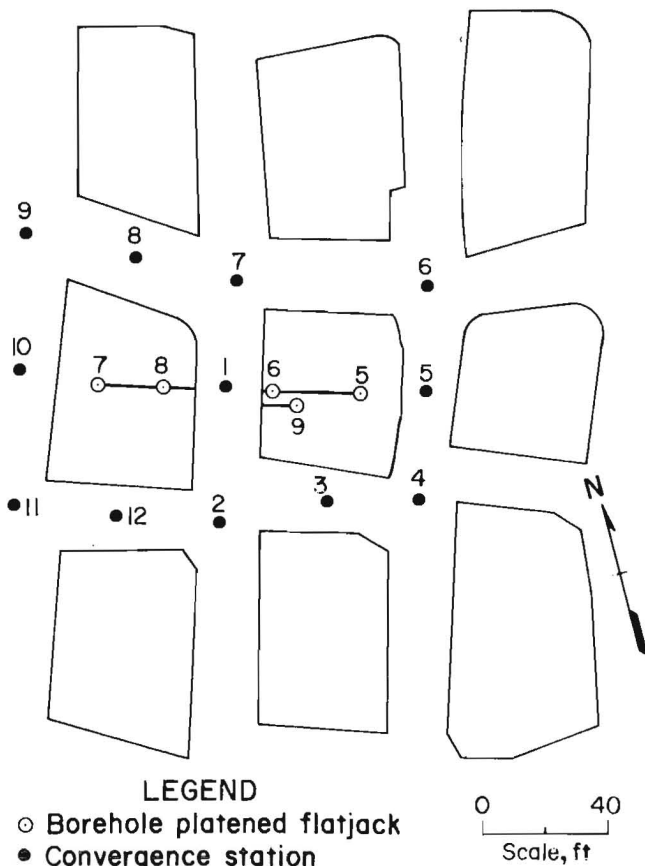
TABLE 2. - Flatjack (BPF) pressures during 177-day
monitoring period, pounds per square inch

BPF	Initial (installation date)	Day 44 (25 pct of total period)	Day 88 (50 pct)	Day 177 (final)
UPPER MINE				
1........	1,100	8,100	8,100	8,100
2........	1,225	950	900	950
3........	1,200	3,175	4,050	5,100
4........	1,275	1,200	1,250	1,250
LOWER MINE				
5........	1,300	1,090	1,050	1,050
6........	1,000	880	850	850
7........	1,300	1,050	1,000	1,050
8........	1,300	900	900	900
9........	1,200	1,000	1,000	950

TABLE 3. - Results of convergence monitoring in upper mine, inches

Station	Day 44	Day 88	Day 177 (final)	Station	Day 44	Day 88	Day 177 (final)
1..............	1.40	1.95	3.54	7..............	1.15	1.85	3.00
2..............	.84	1.25	2.13	8..............	.81	1.26	2.08
3..............	ND	ND	ND	9..............	2.23	3.26	5.00
4..............	.60	1.29	[1]1.80	10..............	.94	1.31	2.12
5..............	1.24	1.88	2.71	11..............	.80	1.13	1.92
6..............	1.32	2.03	3.37	12..............	1.40	1.45	2.24

ND No data because station was destroyed.
[1]Monitoring discontinued on day 134 due to bad roof conditions.

pressure throughout the study. BPF 1, installed at 1,100 psig, increased to 4,500 psig 16 days into the study. BPF 3, installed at 1,200 psig, increased to 2,500 psig, also 16 days into the study. Total pressures recorded from BPF 1 and 3 were 8,100 and 5,100 psig respectively, resulting in pressure increases of 7,000 and 3,900 psig. Note that any increases in pillar pressure for the upper mine were from BPF's installed within the core of the instrumented pillars. The BPF's located at 10-ft depths showed no major increases in pressure. Figure 19 represents a graph of pressure increases versus time for all BPF's installed in the upper mine. No major increases in pillar pressure were recorded from BPF's installed in the lower mine. Increases in core pressure and how this relates to conditions will be discussed in the Innerburden Pressure and the Floor Heave Analysis sections.
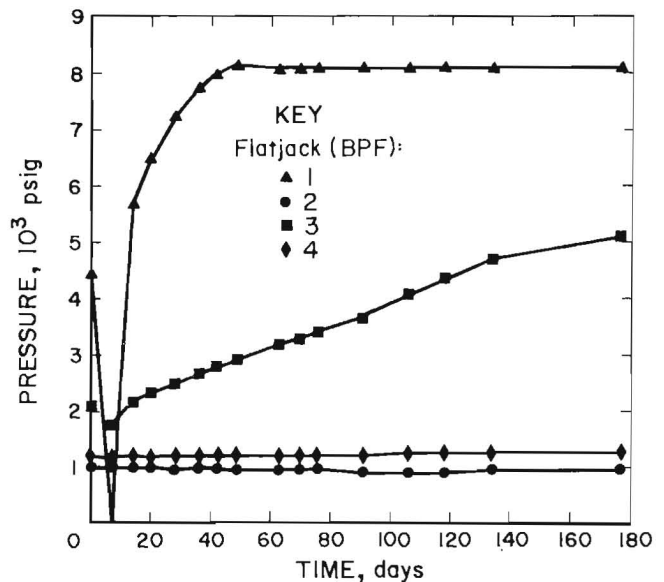

FIGURE 19.—Pressure increase versus time in upper mine.

17

Tables 3 and 4 present measured convergence recorded for the upper and lower mines, respectively. Monitoring of all convergence stations within both mines was also performed at least once a week. Maximum convergence of 5 in occurred at station 9, which is located in the track entry within the upper mine. Roof to floor convergence within the upper mine increased very rapidly. Measurements performed showed an average of 0.5 in of closure every month. No major roof to floor convergence was measured within the lower mine. Figures 20, 21, and 22 show total convergence within the upper mine for 44 days, 88 days, and 177 days. Note the trend of movement with respect to figure 22. Major movement occurred outby and in a southwest direction in relation to the instrument array. Figure 23 displays total convergence versus time for the four convergence stations located along this trend of major roof to floor

TABLE 4. - Final convergence monitoring results for lower mine, inches

Station	Final measurement (177 days)
1.....................	0.05
2.....................	.04
3.....................	0
4.....................	0
5.....................	0
6.....................	0
7.....................	.11
8.....................	.05
9.....................	.01
10....................	0
11....................	.13
12....................	.04

NOTE.--Major movement occurred within the lower mine.

LEGEND

—1.5— Convergence contour line; contour interval 0.5 in

• Convergence station

0   40
Scale, ft
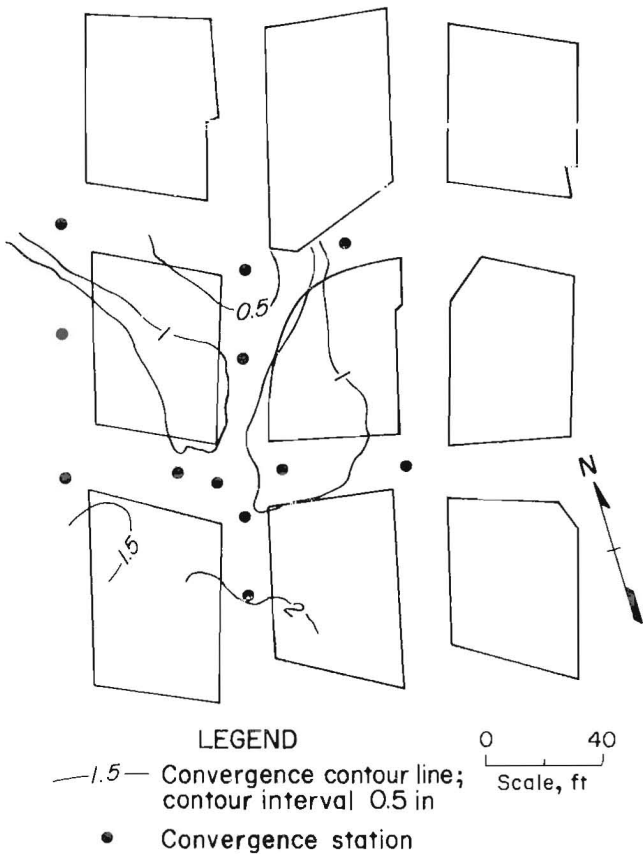
FIGURE 20.—Upper mine convergence contours after 44 days of monitoring.

—2.5— Convergence contour line; contour interval 0.5 in

• Convergence station

0   40
Scale, ft
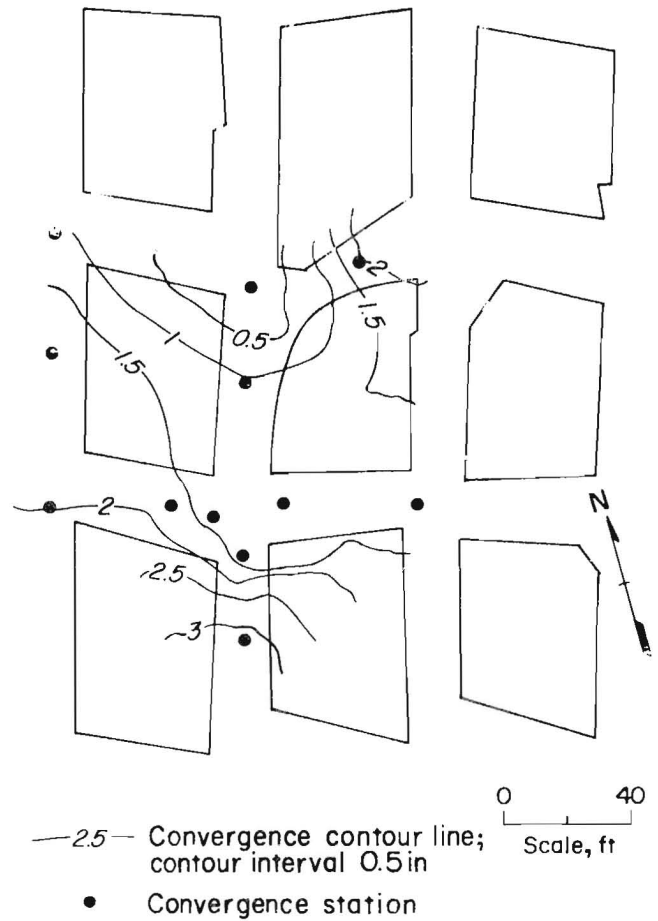
FIGURE 21.—Upper mine convergence contours after 88 days of monitoring.

FIGURE 23.—Total convergence versus time in upper mine.

LEGEND

—*1.5*— Convergence contour line;
contour interval 0.5 in
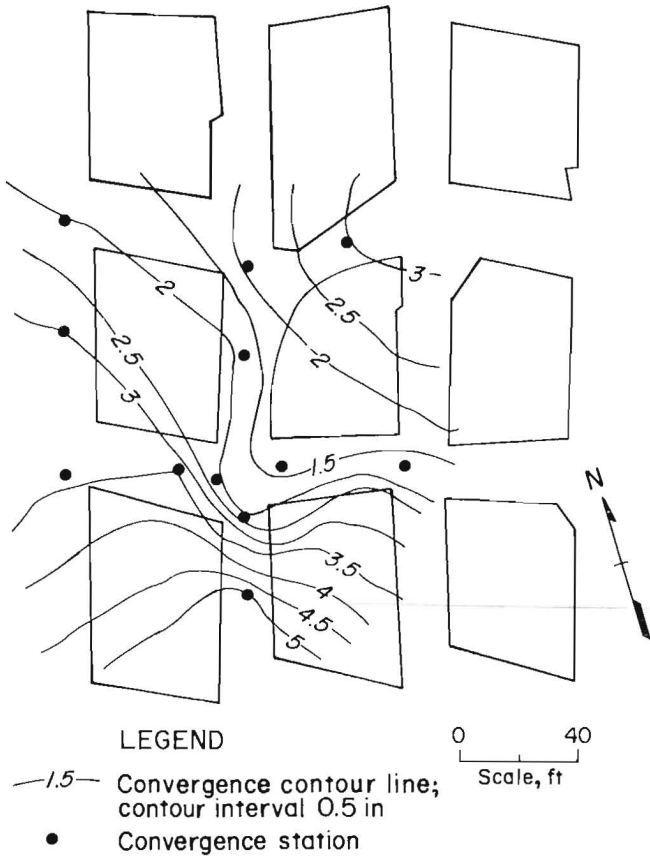
● Convergence station

0   40
Scale, ft

FIGURE 22.—Upper mine convergence contours after 177 days of monitoring.

movement. Roof to floor convergence monitored in the lower mine was limited. Most movement that occurred was 0.13 in at station 11. Figure 24 represents total convergence (177 days) monitored within the lower mine.

Innerburden Pressure Analysis

Utilizing the model developed by Peng and Chandra (13), a stiff-pillar analysis is used to calculate innerburden pressure between superimposed workings. In stiff-pillar analysis, the pillar is assumed to bear the weight of the overburden until failure, at which point the pillar loses all support capacity. The vertical overburden load is uniformly distributed on pillars, and the pillar pressure is estimated using the TAM:

$$P_p = dp \, (1/1-R), \qquad (3)$$

LEGEND
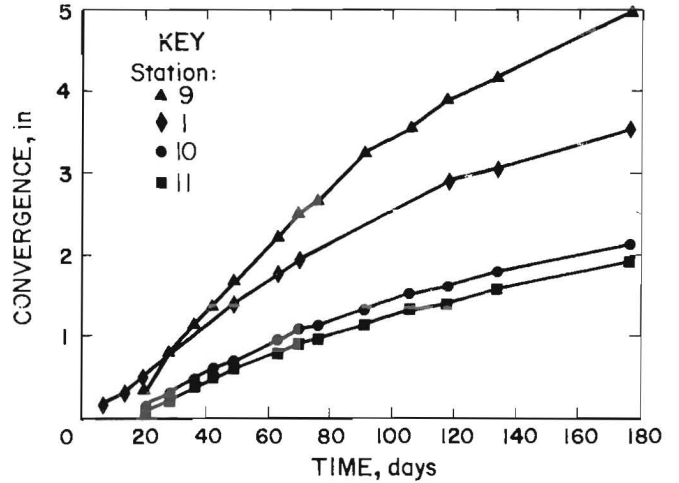
—*0.1*— Convergence contour line;
contour interval 0.5 in
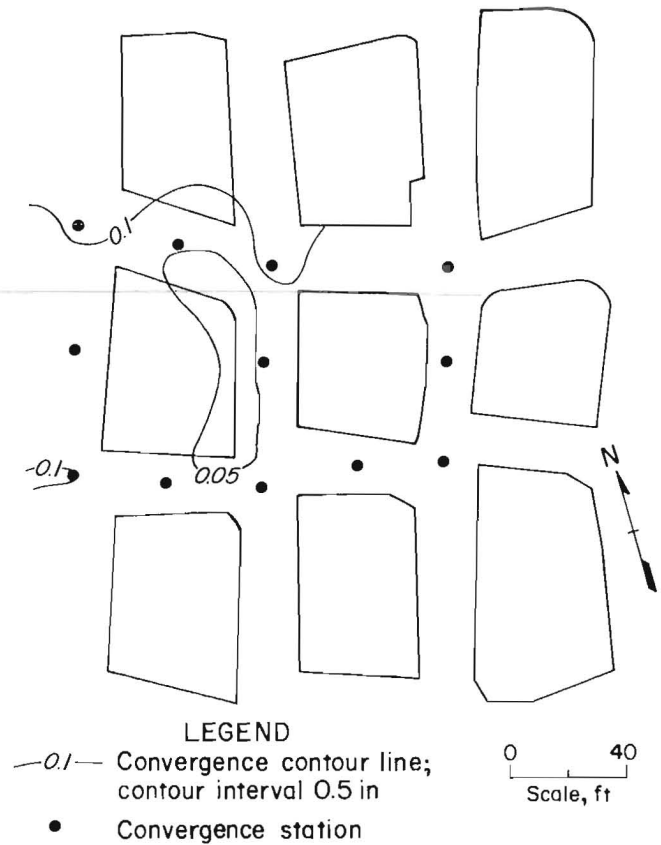
● Convergence station

0   40
Scale, ft

FIGURE 24.—Lower mine convergence contours after 177 days of monitoring.

where P_p = vertical pillar pressure, psi,

  d = depth, ft,

p = 1.1 psi/ft of overburden,

and R = extraction ratio.

The pressure at any point in the inner-burden between two superimposed pillars can be represented by the equation

$$P_I = P_{pu} (2z/W_{pu}) + P_{pl} (2z/W_{pl}), \quad (4)$$

where P_I = innerburden pressure, psi,

P_{pu} = vertical pillar pressure, upper mine, psi,

P_{pl} = vertical pillar pressure, lower mine, psi,

W_{pu} = width of pillar, upper mine, ft,

W_{pl} = width of pillar, lower mine, ft,

x = change in horizontal distance, ft,

z = change in vertical distance in innerburden, ft,

and $x = z$ in relation to figure 16.

The quantities $(2z/W_{pu})$ and $(2z/W_{pl})$ are defined as the influence bulbs, as shown in figure 16.

The following two equations can be used to calculate the pillar pressure in the upper and lower mines.

Upper mine: d = 960 ft, R = 0.50,

$$P_{pu} = dp (1/1-R),$$

$$= (960 \text{ ft}) (1.1 \text{ psi/ft}) (1/1-0.50),$$

$$= 2,110 \text{ psi}. \quad (5)$$

Lower mine: d = 1,000 ft, R = 0.50,

$$P_{pl} = dp (1/1-R),$$

$$= (1,000 \text{ ft}) (1.1 \text{ psi/ft}) (1/1-0.50),$$

$$= 2,200 \text{ psi}. \quad (6)$$

By substituting P_{pu} and P_{pl} into equation 4, the vertical pressure at the midpoint (z = 20) of the innerburden is calculated (P_I) as

$$P_I = P_{pu} (2z/W_{pu}) + P_{pl} (2z/W_{pl}),$$

$$= 2,110 (40/55) + 2,200 (40/55),$$

$$= 2,110 (0.72) + 2,200 (0.72),$$

$$= 2,110 (0.85) + 2,200 (0.85),$$

$$= 3,665 \text{ psi} \quad (7)$$

(Note: From figure 16 ([13]), the influence bulb is approximately 0.85.)

The innerburden stress factor (ISF) is defined as the innerburden pressure (after mining) at any point divided by the superincumbent pressure (before mining) at the same point or

$$ISF = P_I /(1.1 \text{ psi/ft}) (d), \quad (8)$$

where at the innerburden midpoint, depth = 980 ft,

and ISF = 3,665 psi/(1.1 psi/ft) (980 ft),

$$= 3.4.$$

Owing to the ground conditions present in the study area, it can be assumed that the innerburden pressure and the corresponding ISF are much higher. Using the peak pressures obtained from the BPF's, these values can be estimated.

The increase in pillar pressure, as recorded from BPF pressure readings, is represented as

$$B_p = P_p + (BPF_p - P_p) K, \quad (9)$$

where B_p = increase in pillar pressure, psi,

P_p = pillar pressure by TAM, psi,

BPF_p = peak BPF pressures, psi,

and   K = K factor.[4]

The following two equations can be used to calculate the increase in pillar pressure in the upper and lower mines.

Upper mine peak pressure: 8,100 psig,

$$B_{pu} = P_{pu} + (BPF_p - P_{pu}) K,$$

$$= 2,110 + (8,100 - 2,110) (0.75),$$

$$= 2,110 + 4,490,$$

$$= 6,600 \text{ psi}. \tag{10}$$

Lower mine peak pressure: 1,050 psig,

$$B_{pl} = P_{pl} + (BPF_p - P_{pl}) K,$$

$$= 2,200 + (1,050 - 2,200) (0.75),$$

$$= 2,200 + 0^4,$$

$$= 2,200 \text{ psi}. \tag{11}$$

By substituting B_{pu} and B_{pl} for P_{pu} and P_{pl} in equation 4, the vertical pressure at the midpoint (z = 20) of the innerburden (P_I) is calculated as

$$P_I = B_{pu} (2z/W_{pu}) + B_{pl} (2z/W_{pl}),$$

$$= 6,600 (40/55) + 2,200 (40/55),$$

$$= 6,600 (0.72) + 2,200 (0.72),$$

$$= 7,480 \text{ psi}. \tag{12}$$

The ISF is calculated as

$$ISF = 7,480 \text{ psi}/(1.1 \text{ psi}) (980 \text{ ft}),$$

$$= 6.9. \tag{13}$$

(Note: From figure 16 (13) influence bulb is approximately 0.85.)

---

[4]The K factor at 1,200 psi setting pressure is 0.75. The K factor relates BPF pressure to actual strata pressure through calibration (14). When $BPF_p < P_p$, use 0.

In reality, the two-dimensional analysis is a simplification of a very complicated stress condition. What this analysis does provide is a method of assessing the mining-induced stress as it relates to overburden depth and innerburden thickness. In the case where innerburden thickness is less than two pillar widths, a high-stress condition can exist and could cause ground instability depending on pillar and entry design and the in situ strength of the surrounding strata. At the study site, overburden was a maximum (1,000 ft) and innerburden a minimum (40 ft) over the entire coal property. The ISF was calculated to be almost seven times the superincumbent pressure (before mining), which might possibly have led to both entry and pillar instability. In areas of decreased overburden and increased innerburden, the ISF should be less, resulting in more stable ground conditions.

Floor Heave Analysis

Pressure-bulb analysis can also be used to assess the stress distribution within the floor. Figure 25 shows a scale drawing of the study area and the load distribution on the two instrumented pillars in the upper mine. The vertical
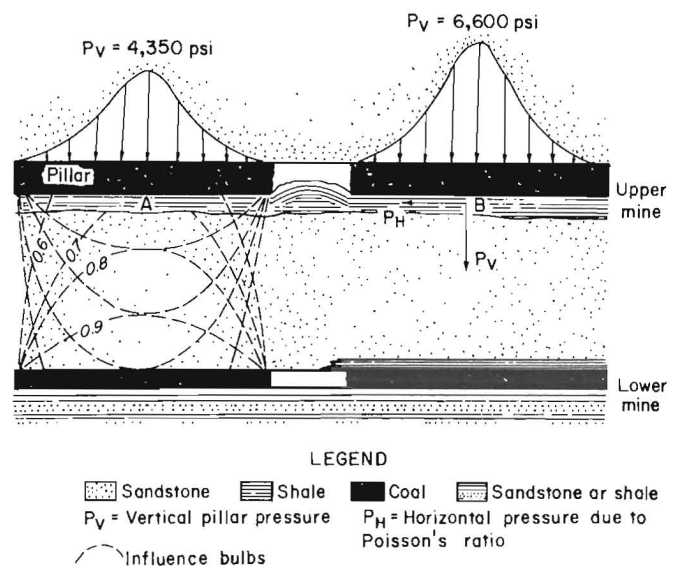
FIGURE 25.—Load distribution on instrumented pillars in upper mine.

pressure is calculated according to equation 14.

$$P_v = P_p + (BPF_p - P_p) K, \qquad (14)$$

where P_v = vertical pillar pressure, psi,

P_p = pillar pressure by TAM, psi,

BPF_p = peak BPF pressure, psi,

and K = factor.[5]

Peak BPF pressure for pillar on left side (fig. 25) was 5,100 psig at 30 ft. Therefore, from equation 13

$$P_v = P_p + (BPF_p - P_p) K,$$

$$= 2,110 + (5,100 - 2,110) (0.75),$$

$$= 4,350 \text{ psi}, \qquad (15)$$

and peak BPF pressure in pillar on right side (fig. 25) is 8,100 psig at 30 ft.

$$P_v = P_p + (BPF_p - P_p) K,$$

$$= 2,110 + (8,100 - 2,110) (0.75),$$

$$= 6,600 \text{ psi}. \qquad (16)$$

BPF readings show that load distribution on the pillar resembles that of a peak load towards the core of the pillar with decreasing load outwards. This core loading is characteristic of a stiff pillar approaching failure. The ribs fail owing to the lack of horizontal confinement as the overburden load continues to be supported by the pillar core. Eventually, the load exceeds the strength of the pillar and it fails, losing all support capacity. But, in this case, a soft floor material (shale) does not provide ample bearing support and fails before the pillar. The failure is experienced as heaving when floor material is pushed aside and upward owing to horizontal stresses associated with

[5]See footnote 4.

pressure-bulb interference. The magnitude of this horizontal stress can be estimated by using innerburden pressure calculations and Poisson's ratio.

The following two equations can be used to calculate the innerburden pressure at points A and B directly beneath the pillars, as shown in figure 25.

Point A: Using equation 4 (for W_{pu}; z = 0, for W_{pl}; z = 40),

$$P_I = P_{pu} (2z/W_{pu}) + P_{pl} (2z/W_{pl}),$$

$$= 4,350 (0/55) + 2,200 (80/55),$$

$$= 4,350 (0) + 2,200 (1.45),$$

$$= 4,350 (1) + 2,200 (0.7),$$

$$= 5,890 \text{ psi}. \qquad (17)$$

(Note: From figure 16 (13) the influence bulb at 0 is 1, and at $\overline{1.45}$ is approximately 0.7.)

Point B: Using equation 4 (for W_{pu}; z = 0, for W_{pl}; z = 40),

$$P_I = P_{pu} (2z/W_{pu}) + P_{pl} (2z/W_{pl}),$$

$$= 6,600 (1) + 2,200 (0.7),$$

(same influence bulb as point A).

$$= 8,140 \text{ psi}. \qquad (18)$$

The horizontal component of this vertical pressure beneath the pillars can be estimated through Poisson's ratio. In practice, Poissons's ratio is estimated to be 1.0 to 0.3 times the vertical pressure. Using the lower limit, 0.3, P_H at points A and B can be estimated.

Point A:

$$P_H = 0.3 (P_v),$$

$$= 0.3 (5,890 \text{ psi}),$$

$$= 1,770 \text{ psi}. \qquad (19)$$

Point B:

$$P_H = 0.3 \ (P_v),$$

$$= 0.3 \ (8,140 \ psi),$$

$$= 2,440 \ psi. \tag{20}$$

As shown in figure 25, P_H acts perpendicular to the trend of the entry. This heaving mechanism is similar to that of a piercing wedge; i.e., the high vertical load pushes the pillar core downward into the soft floor, and the associated horizontal component pushes the material outward. When considering the entire structure in both mines, the floor of the upper mine is the weakest member of the structure and fails first. Owing to height restrictions, BPF and convergence installations were limited to more stable areas in the lower mine, and those pillars have not shown similar core loading. It can be assumed that in unstable areas of the lower mine, the same heaving analysis can be applied.

CONCLUSIONS

Based on the information received and collected throughout the study, the following conclusions can be made.

Overburden depth above the study area was approximately 1,000 ft. The overburden depth changed dramatically over the study section and reached a topographic high over the study area. Prior research and other case studies (2) have shown that excessive overburden depths could lead to unstable ground conditions.

Innerburden thickness in the study area was approximately 40 to 45 ft, less than one pillar width. Prior research has shown (2) that workings in close proximity, less than two pillar widths, may create ground control problems above and below workings.

Previous research showed (2) that innerburden material, comprised mostly of sandstone, dampened the effects of pillar load transfer. Sandstone at the study area comprised 77 pct of the innerburden. According to Haycocks (2), this percentage requires 78 ft of innerburden for stable conditions.

Heaving was experienced in both the sandstone and the shale floor units. The shale floor, being a low-modulus material, resulted in "hump-like" floor heave, whereas the sandstone floor, being a high-modulus material, resulted in a "buckling" type of floor heave.

To minimize interaction effects, optimum seam sequencing would mean mining the upper seam first to total extraction, then continuing downwards. In this case, the upper seam pillars were developed first, with lower seam pillars developed approximately 2 yr later.

Superpositioned pillars are a conventional engineering practice in multiple-seam design. This practice was followed, but mine overlays show pillars and entries were not totally superpositioned.

The BPF pressure readings in the upper mine showed a core loading characteristic of a stiff pillar approaching failure. These pressures were not measured in the instrumented pillars in the lower mine because drilling equipment restrictions limited instrument installation to the more stable mine areas.

Average convergence in the upper mine entries was 2.50 in, as compared to the lower mine entries averaging 0.04 in. This difference was due to drilling equipment restrictions in the lower mine that limited instrument installation to a more stable mine area.

The ISF was a function of pillar width, innerburden thickness, and depth. This factor, as calculated through BPF pressure readings and using pressure-bulb analysis (13), showed that vertical pressure was over seven times the superincumbent pressure.

REFERENCES

1. Haycocks, C., B. L. Ehgartner, M. Karmis, and E. Topuz. Pillar Load Transfer Mechanisms in Multi-Seam Mining. Soc. Min. Eng. AIME preprint 82-69, 1982, 6 pp.

2. Haycocks, C., and M. Karmis. Ground Control Mechanisms in Multi-Seam Mining. BuMines OFR 7-84, 1983, 328 pp.

3. Ehgartner, B. L. Pillar Load Transfer Mechanisms in Multi-Seam Mining. M.S. Thesis, VA Polytech. Inst. and State Univ., Blacksburg, VA, 1982, 85 pp.

4. Finlay, J., and A. Winstanley. The Interaction of Longwall Workings. Trans. Inst. Min. Eng., v. 87, 1934, pp. 172-189.

5. Hasler, H. Simultaneous vs Consecutive Workings of Coal Beds. Trans. Soc. Min. Eng. AIME, v. 3, No. 5, 1951, pp. 436-440.

6. Stemple, D. A Study of Problems Encountered in Multiple-Seam Coal Mining in the Eastern United States. VA Polytech. Inst. Bull., v. 49, No. 5, 1956, p. 65.

7. Lazer, B. Mining Seams Above Mined-Out Lower Seams. Min. Eng. (N.Y.), v. 17, No. 9, 1965, pp. 75-77.

8. Zacher, F. Some Effects of Sewickley Seam Mining on Late Pittsburgh Seam Mining. Trans. Soc. Min. Eng. AIME, v. 4, No. 7, 1952, pp. 687-692.

9. Peperakis, J. Multiple Seam Mining With Longwall. Min. Congr. J., v. 54, No. 1, 1968, pp. 27-29.

10. National Coal Board. Report on the Effects of Working in Adjacent Seams Upon New Developments. Trans. Inst. Min. and Metall., v. 113, 1954, pp. 398-415.

11. Spedding, M. Multiple Seam Mining. Paper in 17th Symposium on Rock Mechanics. Univ. UT, Snowbird, UT, 1976, pp. 22-27.

12. Wilson, J. W., B. D. Singh, and S. Nakajima. Design Considerations for Mining Thick Seams and Seams Lying in Close Proximity to One Another. Paper in 17th Symposium on Rock Mechanics. Univ. UT, Snowbird, UT, 1976, pp. 1B1-1 to 1B1-11.

13. Peng, S., and U. Chandra. Getting the Most From Multiple-Seam Reserves. Coal Min. and Process., v. 17, No. 11, 1980, pp. 78-84.

14. Bauer, E., G. Chekan, and J. L. Hill III. A Borehole Instrument for Measuring Mining-Induced Pressure Changes in Underground Coal Mines. Paper in 26th U.S. Symposium on Rock Mechanics. SD Sch. Mines and Technol., Rapid City, SD, 1985, pp. 1075-1084.